



Contents lists available at ScienceDirect

## Quaternary International

journal homepage: [www.elsevier.com/locate/quaint](http://www.elsevier.com/locate/quaint)

# A multi-proxy record of environmental changes during the Holocene from the Haolaihure Paleolake sediments, Inner Mongolia



Jin Liu <sup>a, b, c, d</sup>, Yang Wang <sup>c, d, e, \*</sup>, Yong Wang <sup>a, \*\*, d</sup>, Youyi Guan <sup>f</sup>, Jin Dong <sup>a</sup>, Tingdong Li <sup>a</sup>

<sup>a</sup> Institute of Geology, Chinese Academy of Geological Sciences, Beijing, 100037, PR China

<sup>b</sup> China University of Geosciences, Beijing, 100083, PR China

<sup>c</sup> Department of Earth, Ocean, and Atmospheric Science, Florida State University, Tallahassee, FL, USA

<sup>d</sup> High National Magnetic Field Laboratory, Tallahassee, FL, USA

<sup>e</sup> Institute of Hydrobiology, The Jinan University, Guangzhou, Guangdong Province, 510632, PR China

<sup>f</sup> Hubei Earthquake Administration, Wuhan, Hubei Province, 430071, PR China

## ARTICLE INFO

### Article history:

Received 7 June 2016

Received in revised form

1 December 2016

Accepted 8 December 2016

Available online 1 March 2017

### Keywords:

Stable isotopes

Holocene paleoclimate

Asian Summer Monsoon

Haolaihure Paleolake

Climate event

## ABSTRACT

The east Central Inner Mongolia is located near the present-day limit of the Asian Summer Monsoon (ASM) influence and therefore sensitive to both regional and global climate change. Here, we present the high-resolution proxy record of regional paleoclimate evolution over the past 12.2 cal ka BP, based on analyses of grain size and organic geochemical proxies (i.e., TOC, TN, C/N,  $\delta^{13}\text{C}$  and  $\delta^{15}\text{N}$ ) preserved in sediments from the Haolaihure Paleolake. The multi-proxy record reveals a cool and dry period from 12.2 to 8.7 cal ka BP and a relatively warm and wet stage from 8.7 to 2.2 cal ka BP, interrupted by a short interval of reduced precipitation at 4.6–3.7 cal ka BP. After 2.2 cal ka BP, the regional environment deteriorated as climate shifted to generally cooler and drier conditions in the area, with a brief return to a warm and wet climate during the Medieval Warm Period. The record also indicates severe drought in the region during the Younger Dryas event. Comparison with other proxy paleoclimate records in Inner Mongolia, South China and central Asia suggests that the environmental conditions in the east central Inner Mongolia were primarily controlled by the ASM in the early to mid-Holocene while the Westerlies appeared to be a major driver of environmental changes in the late Holocene. Six of the eight cool and dry events recorded in Haolaihure Paleolake sediments are in phase with the ice-rafting events in the North Atlantic, and were possibly caused by weakening of both the ASM and the Westerlies.

© 2017 Elsevier Ltd and INQUA. All rights reserved.

## 1. Introduction

The Westerlies and the Asian Monsoon (AM) are two major climate systems influencing the environmental conditions in China. The Westerlies provide a major source of atmospheric moisture (originating from the North Atlantic) for the arid northwestern region of China (Wang et al., 2005a; Chen et al., 2008). The Asian Summer Monsoons (ASM), including East Asian Summer Monsoon (EASM) and Indian Summer Monsoon (ISM), bring warm and moist air from tropical oceans to inland and provide the much needed precipitation to the south and east China during summer months.

\* Corresponding author. Department of Earth, Ocean, and Atmospheric Science, Florida State University, Tallahassee, FL, USA.

\*\* Corresponding author. Institute of Geology, Chinese Academy of Geological Sciences, Beijing, 100037, PR China.

E-mail addresses: [ywang@magnet.fsu.edu](mailto:ywang@magnet.fsu.edu) (Y. Wang), [wangyong@cags.ac.cn](mailto:wangyong@cags.ac.cn) (Y. Wang).

The position of ASM limit is controlled by the ASM strength and varies on various time scales in response to changes in global climate (Yang et al., 2015). The decadal mean locations of the ASM limit for 1968–1978 and 1978–1998, determined from the modern meteorological data (Qian et al., 2007), were approximately along the Great Khingan Mountain and the central and eastern Inner Mongolia (Fig. 1A). The transitional zone between the Westerlies and ASM regimes is particularly sensitive to climate change. Although many studies have investigated the paleoenvironment in the region (Xiao et al., 2006; Chen et al., 2010; Chu et al., 2014; Tang et al., 2015; Zhang et al., 2016), long-term climatic history in this region remains poorly understood. Some studies suggested that the humid condition occurred in the mid-Holocene (Feng et al., 2006; Xiao et al., 2006; Wang et al., 2013a), while others thought that the region was humid in early and mid-Holocene (Jiang et al., 2006, 2010; Wang et al., 2012). The controversies over both the timing and duration of the Holocene climatic optimum may be partly caused by the uncertainties in proxy interpretation and dating and

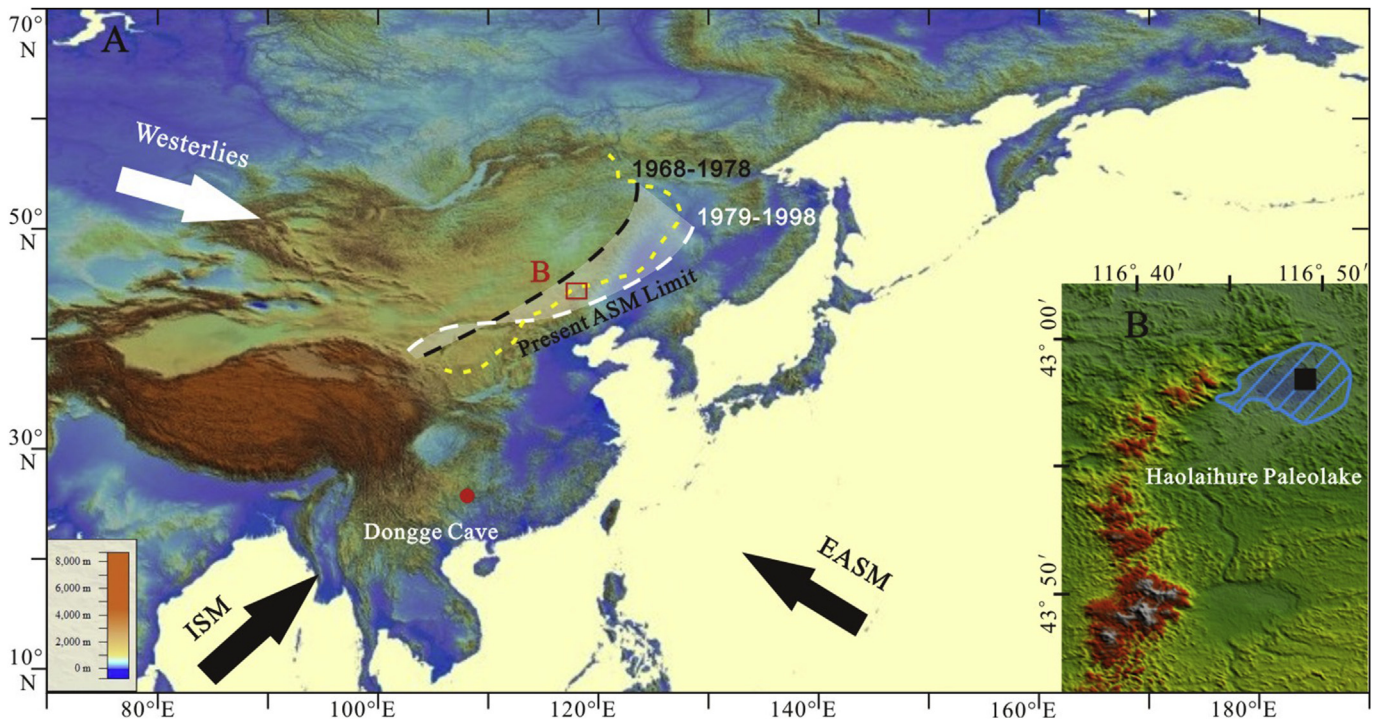


**Fig. 1.** Location of the Haolaihure Paleolake and dominant circulation systems in China. The dash lines represent decadal mean locations of the ASM limit for the year 1968–1978 (black) and 1978–1998 (white), respectively (from Qian et al., 2007). The yellow dash line is the boundary of modern vegetation zone between warm-temperate broadleaved deciduous forest and steppe (Sun and Wang, 2005). (For interpretation of the references to colour in this figure legend, the reader is referred to the web version of this article.)

by differences in geographic locations of the various proxy records (Tang et al., 2015). Moreover, high-resolution paleoclimate records from ice cores, tree rings, speleothems and marine sediments from other parts of the world have revealed abrupt changes in climate over the 13,000 years (Stuiver et al., 1995; Bond et al., 1997; Cheng et al., 2006). But, only a few climatic events have been noted in the Westerlies-ASM transitional zone due to the relatively low resolution of the existing paleoclimate records (Wang et al., 2001; Liu et al., 2002; Sun et al., 2006). Well-dated high-resolution records from this transitional region are needed to provide detail information about paleoenvironmental conditions, and to help fully understand the regional climate history and offer an insight into future climate changes (An et al., 2000).

In this paper, we present a well-dated lacustrine sediment record from the Haolaihure Paleolake in east Central Inner Mongolia located in the Westerlies-ASM transitional zone. The new record spans a time interval from 12.2 cal ka BP (thousands of calibrated years before present; 0 years BP = 1950 CE) to the present, with a resolution of ~22 years. Grain size character and organic geochemical signatures of the sediments, including percentage contents and isotope ratios of carbon (C) and nitrogen (N) and (C/N)<sub>atomic</sub> ratio, were examined to reveal the past changes in environmental conditions in the area. The results were compared with other paleoclimate records in China as well as the record of ice-rafting events in the North Atlantic region to elucidate the possible drivers of environmental changes in the region.

## 2. Study area

The study section of the Haolaihure Paleolake (42°57'2''N, 116°47'37''E, 1295 m above sea level, m a.s.l.) is located in the southeastern Otindag Desert in the east Central Inner Mongolia, China (Fig. 1). The paleolake has dried out and since been covered by an eolian sand layer. The present-day climate in the area is

characterized by a dry windy spring, a wet short summer and a cold long winter (Li, 1993). The average annual temperature is 0–1 °C, with the highest of ~16 °C in July and the lowest of ~-23 °C in January; the annual precipitation is ~250 mm concentrated in July and August brought by the ASM, and evapotranspiration is more than 1300–1900 mm (Li, 1993). The area is in the ASM-Westerlies transitional zone and also in the transition region of modern vegetation zones, with the temperate deciduous and mixed forest biomes in the south and east and temperate steppe in the north and west (Liu, 1988; Sun and Wang, 2005) (Fig. 1). The area around the lake is dominated by a mosaic of *Artemisia–Betula–Chenopodiaceae* woodlands and grasslands. A mixture of *Betula–Pinus–Artemisia* and *Betula–Artemisia* woodlands and grasslands are distributed in the Great Khingan Mountain in the east, and *Artemisia–Chenopodiaceae* steppe in the west (Liu et al., 2002).

## 3. Materials and methods

### 3.1. Lithology and chronology: radiocarbon and OSL

The Haolaihure profile is 545 cm thick and can be divided into five sections based on the lithology: (1) light green clay from 545 to 503 cm depth, with a light grey fine sand layer at 526–514 cm depths; (2) black clay with lamination from 503 cm to 406 cm; (3) dark grey clay with lamination from 406 cm to 210 cm; (4) light grey clay from 210 cm to 30 cm; (5) light yellow fine sand from 30 cm to 0 cm.

Since no visible terrestrial plant debris was found in the lake sediment layer, we collected a total of 12 bulk organic matter (OM) samples from the strata with relatively abundant organic materials for accelerator mass spectrometry (AMS) <sup>14</sup>C dating. Three of them (HL12-35, HL12-40, HL12-70) were measured at Beta Analytic Inc., Miami, USA, and the rest of the samples were analyzed in the Institute of Heavy Ion Physics School of Physics at Peking University,

Beijing, China.

In addition, a sand sample was collected from 523 cm depth in the profile for optically stimulated luminescence (OSL) dating to independently test radiocarbon-based chronologies (Lukas et al., 2012; Long et al., 2015). The sand sample was obtained by hammering steel tubes (40 cm long, 5 cm in diameter) into a fresh profile. The tube was covered and sealed with aluminum foil, and then wrapped using black plastic bags and tape to avoid light exposure. The OSL sample was analyzed in the State Key Laboratory of Earthquake Dynamics in Institute of Geology, China Earthquake Administration.

### 3.2. Grain size analysis

A total of 501 samples except the sand layers at 0–30 cm and 514–526 cm depths were analyzed for grain size character. 10–20 ml of 30% H<sub>2</sub>O<sub>2</sub> and 10–15 ml 10% HCl were used to remove the organic matter and carbonate, respectively. The treated samples were rinsed at least three times with deionized water until they were neutral. Afterwards, 10 ml of 0.05 M (NaPO<sub>3</sub>)<sub>6</sub> were added to each sample. The samples were then placed in an ultrasonic vibrator for 15 min to disperse the sediment. The grain-size distribution was measured using a Malvern Mastersizer 2000 laser grain-size analyzer with a measurement range of 0.02–2000 μm. Each sample was analyzed twice, and the relative error was always less than 2%. Because of its relatively high hardness and chemical stability, quartz surface features can yield clues to the sedimentary environment and degree of processing during transport (Krinsley and Margolis, 1969). The surface characters of the sand grains in the thick sand layer at 514–526 cm depths were examined under an electron scanning microscope (ESM) at Chinese Academy of Geological Sciences to infer the depositional environment.

### 3.3. Geochemical analysis

The amount and geochemical signatures of OM in lacustrine sediments may be used to deduce information about lake productivity and origin of OM and to infer paleoenvironmental conditions (Meyers, 1997; Das et al., 2013; Lorente et al., 2014). The sediment samples were collected at 1 cm interval from the surface to the base of the profile for elemental and isotope analyses. The samples were homogenized into a fine powder first. Subsamples (~1 g sediment) were subjected to 0.5 M HCl overnight to remove carbonate. After washing with deionized water to neutral pH, the samples were freeze-dried. About 5–35 mg of each dried sediment sample was then packed into a tin cup for analyses of percentage contents of total organic carbon (TOC) and organic nitrogen (TN) as well as stable carbon and nitrogen isotope ratios.

Sediment samples were analyzed using a Carlo Erba Elemental Analyzer (EA) connected to a Thermo Finnigan MAT Delta Plus XP stable isotope ratio mass spectrometer (IRMS) through a ConFlo III interface at the Florida State University. At least two sets of five different laboratory standards of known elemental and isotopic compositions, including YWOMST-1 (cane sugar), YWOMST-2 (phenylalanine), YWOMST-3 (L-phenylalanine), YWOMST-5 (urea) and Urea-2, were analyzed with each batch of samples. Additionally, a blank (empty tin cup) was run, along with each batch of samples, to ensure that there was no residual gas contamination or memory effect. The isotope results are reported in the standard delta (δ) notation in per mil as δ<sup>13</sup>C values with reference to the international VPDB standard and δ<sup>15</sup>N values with reference to AIR. The precision of the C and N isotope analysis is ±0.2‰ or better, for TOC and TN are 3% and 1%, respectively.

## 4. Results

### 4.1. Chronology

The AMS (accelerator mass spectrometry) <sup>14</sup>C dates, obtained from bulk organic matter from organic-rich layers at various depths, are listed in Table 1. Additionally, one OSL date was collected from the fine sand layer at 523 cm depth. Nine <sup>14</sup>C dates analyzed in the Peking University and the OSL date have been reported in our previous studies by Guan et al. (2010). Both the OSL date of the eolian sand (11.6 ± 1.6 ka) and the <sup>14</sup>C date of bulk organic matter (12.86 ka BP) right below the sand layer (Table 1) indicate that the sand layer (occurring at 526–514 cm depth) was most likely deposited during the Younger Dryas (YD) event (Stuiver et al., 1995; Bond et al., 1997; Muscheler et al., 2008). The YD cooling event has been documented in lake sediments in Inner Mongolia (Wang et al., 1994; Chen et al., 1996). We therefore correlate this sand layer to the YD event (Fig. 4). The radiocarbon dates of lacustrine sediments in the arid–semiarid region of China are generally affected by <sup>14</sup>C reservoir effect (Liu et al., 2008; Ren, 1998). To assess the magnitude of the old carbon effect, we extrapolated the AMS <sup>14</sup>C dates at 438 cm and 473 cm depths to 514 cm depth where the boundary between the sand layer and the overlying clay occurs and assume that it represents the date for the end of the YD event in the Haolaihure profile. The extrapolated <sup>14</sup>C date is 12,570 yr BP, which is about 2570 yr older than the actual date for the end of the YD event (i.e., 10,000 yr BP, uncalibrated) (Broecker et al., 1988). Moreover, in the upper half profile, the lacustrine sediments are coarsening upward then overlaid by eolian sediments, indicating the lake experienced a gradually upward shallowing process. And it shows no any traces of obvious erosion and undisturbed between the uppermost eolian sediment and the lower lacustrine sediment (Fig. 2), indicating there is a great reservoir age. Therefore, we regard the 2570 yr as the apparent <sup>14</sup>C reservoir age for the paleolake sedimentary organic matter. This reservoir age is also consistent with the result of Ren (1998) which compared the radiocarbon dates and <sup>210</sup>Pb measurements and suggested nearly 2000 years “hard water” effect in eastern Inner Mongolia.

After deducting the <sup>14</sup>C reservoir age, all radiocarbon dates were calibrated to calendar years before present (cal ka BP) using the Oxcal v 4.2 program (Ramsey, 2009), with the IntCal 13 data set (Reimer et al., 2013) (Table 1). Then the age–depth model was derived based on linear interpolation of two adjacent calibrated median <sup>14</sup>C ages (Fig. 2), assuming a constant sedimentary rate between two control points. Although there might be large difference in deposition rate between lacustrine sediment and eolian sand, the relatively constant deposition rate between the three radiocarbon dates in the bottom indicate that the deposition difference during this period is not great.

### 4.2. Grain size character

Eolian sediment typically consists of rounded sand grains, along with numerous craters of variable geometry on their surfaces, apparently due to turbulent collisions during transport (Mahaney, 2002). Examination under an ESM reveals that medium-fine sands in the 526–514 cm depth interval are rounded grains, with irregular impact pits (Fig. 3), indicating an eolian environment. The grain character is also consistent with modern eolian sand in the Qaidam Basin and Tengger Desert (Dai, 1988). Therefore, the sand layer at 526–514 cm depth is most likely the result of an eolian sand activity and thus indicates dry environment.

Mean grain size (Mz) is used to describe the grain size character

**Table 1**

AMS radiocarbon dates of samples from the Haolaihure Paleolake. All ages were calibrated using Oxcal v 4.2 program (Ramsey, 2009) with IntCal 13 dataset (Reimer et al., 2013).

Lab number	Sample number	Depth (cm)	Dating material	AMS <sup>14</sup> C age ±1σ (yr BP)	<sup>14</sup> C age after deducting the carbon reservoir	Calibrated <sup>14</sup> C age (2σ) (cal yr BP)	Median point (cal yr BP)
BA08866	HL08-30	30	Organic matter	2825 ± 40	255 ± 40	14–455	302
BA08867	HL08-100	100	Organic matter	4995 ± 35	2425 ± 35	2352–2700	2462
BA08868	HL08-155	155	Organic matter	5920 ± 35	3350 ± 35	3480–3688	3591
BA08869	HL08-228	228	Organic matter	6715 ± 40	4145 ± 40	4538–4827	4687
BA08870	HL08-273	273	Organic matter	7710 ± 40	5140 ± 40	5750–5990	5900
Beta - 363610	HL12-35	335	Organic matter	9050 ± 40	6480 ± 40	7310–7470	7381
Beta - 363611	HL12-40	340	Organic matter	9090 ± 40	6520 ± 40	7325–7551	7438
BA08871	HL08-356	356	Organic matter	9395 ± 45	6824 ± 45	7582–7744	7655
Beta - 363,612	HL12-70	370	Organic matter	9640 ± 40	7070 ± 40	7800–7972	7896
BA08872	HL08-438	438	Organic matter	10,865 ± 45	8295 ± 45	9136–9432	9311
BA08873	HL08-473	473	Organic matter	11,650 ± 45	9080 ± 45	10,179–10375	10,234
BA08874	HL08-542	542	Organic matter	12,860 ± 45	10,290 ± 45	11,832–12380	12,070

of the profile (Fig. 4). It varies consistently with lithology, with an average Mz value of 22 μm and an abrupt change occurred at 410 cm depth. Generally, the mean grain size of lacustrine sediment below 410 cm depth is ~17 μm, which is finer than the sediment in the 410–30 cm interval (~24 μm).

4.3. Character of TOC, TN, C/N, and δ<sup>13</sup>C, δ<sup>15</sup>N

The C (and N) content of the eolian sand layer (526–514 cm) near the base of the section, which we correlate to the YD event, is about 0.01% or less, too low to yield a strong enough signal in the mass

spectrometer for accurate isotope measurements. The geochemical results of the rest of the samples display significant variations with depth (Fig. 4).

The bulk organic C and N percentage contents (TOC and TN) in lacustrine sediments are strongly correlated (R<sup>2</sup> = 0.93) and varied from 0.3 to 11.4% and 0.1%–1.04%, respectively (Fig. 4). High TOC and TN values appeared from 411 cm to 36 cm (8.7 cal ka BP to 0.5 cal ka BP), averaging ~7.6% and 0.7%, respectively. Above and below this depth interval, the TOC and TN were at relatively low levels.

The (C/N)<sub>atomic</sub> ratios of the sediments in the profile normally

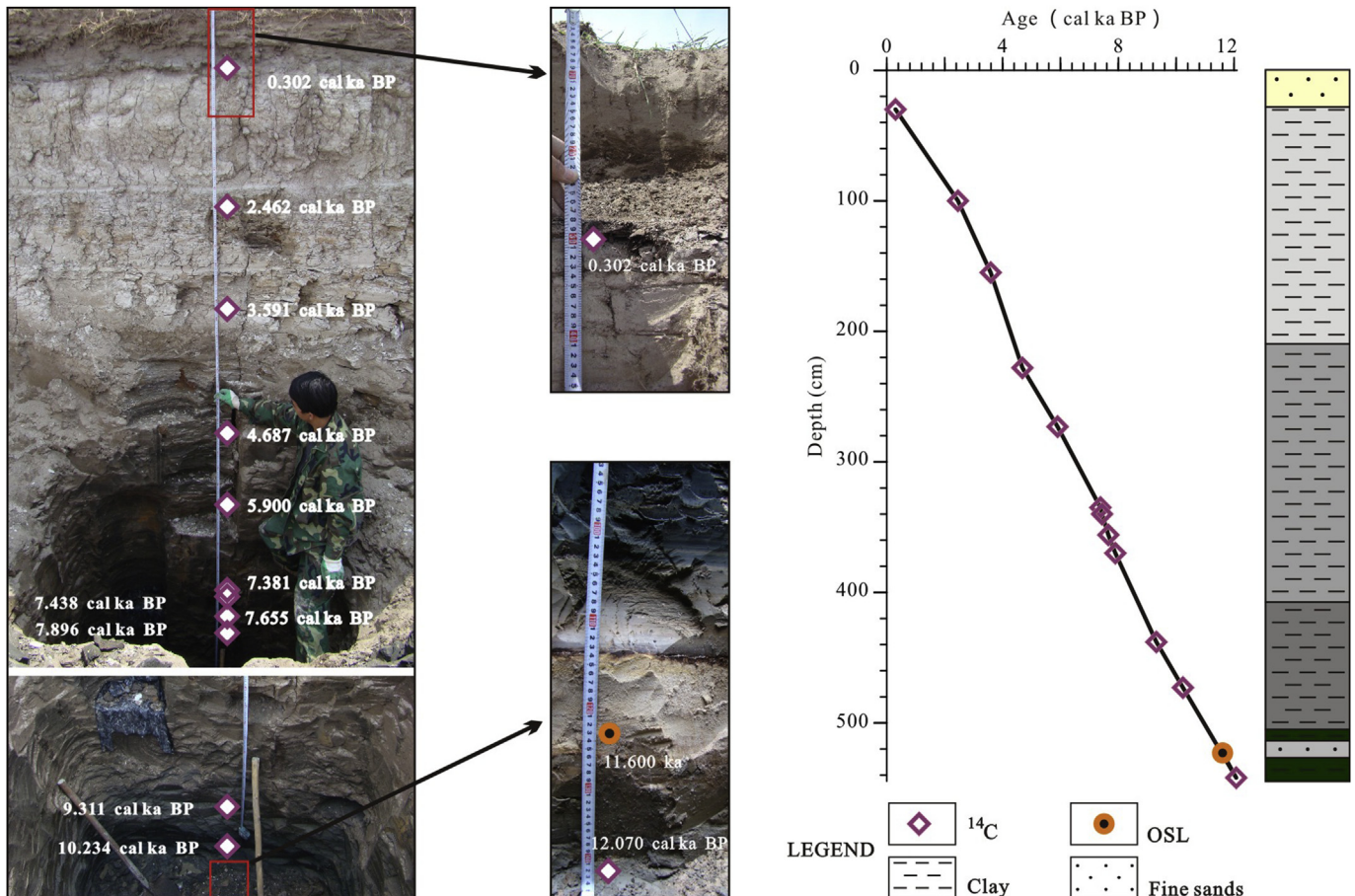


**Fig. 2.** Photograph of the Haolaihure Paleolake profile HL-08 (left) and age–depth model (right). The <sup>14</sup>C ages are converted to cal yr BP using OxCal 4.2 (Ramsey, 2009). The age model was derived from the linear interpolation of the midpoints of the calibrated <sup>14</sup>C dating results (after correction for an apparent reservoir age of 2570 yr).

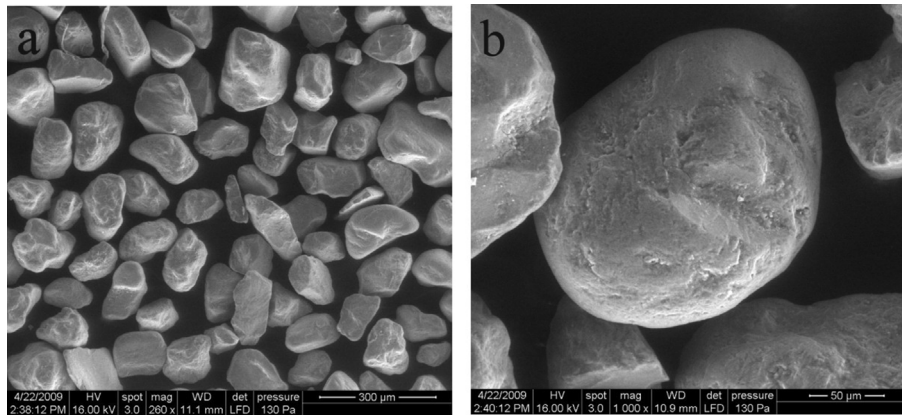


Fig. 3. Photograph of sand grains in the 526–514 cm depth interval by SEM. Rounded grain with irregular impact pits indicates an eolian origin.

vary between 7 and 22, with an average of 12.6 (Fig. 4). The data show a relative high value from 411 cm to 90 cm (8.7–2.2 cal ka BP), and decreasing trends in bottom and top of the profile with extremely high values occurring at 47–30 cm depths (0.8–0.3 cal ka BP).

The  $\delta^{13}\text{C}$  values of bulk sedimentary OM show a broad range of variations mainly between  $-28.0\text{‰}$  and  $-18.0\text{‰}$ , with a gradual positive shift from 514 cm to 90 cm (11.3–2.2 cal ka BP) and an overall negative shift in the late Holocene. There is a prominent positive carbon isotope excursion at 47–30 cm depth interval (0.8–0.3 cal ka BP) (Fig. 4).

The  $\delta^{15}\text{N}$  values of bulk sedimentary OM vary between 1.4‰ and 9‰, showing a gradual increasing trend from 411 cm to 159 cm (8.7–3.7 cal ka BP) and a decreasing trend from 514 to 411 cm (11.3–8.7 cal ka BP) and also from 159 to 96 cm depth (3.7–2.3 cal ka BP). Above 44 cm depth (after 0.7 cal ka BP), there was a sharp increase ( $\sim 7.4\text{‰}$ ) of nearly three folds in  $\delta^{15}\text{N}$  compared with the mean value of the depth interval below ( $\sim 2.5\text{‰}$ ) (Fig. 4).

## 5. Paleoenvironment reconstruction and comparison

### 5.1. Proxy interpretation

The grain-size distribution of lake sediments, which reflects the dynamics of sediment transport and deposition, has been widely used for paleoenvironmental reconstruction (Håkanson and Jansson, 1983; Xiao et al., 2009). Coarse clastic materials usually indicate high transport energy. In general, an increase in regional precipitation resulting from a shift to wetter climatic conditions could strengthen the regional hydrodynamics and erosion intensity of the watershed, leading to coarser clastic deposits in the lake (Håkanson and Jansson, 1983; Campbell, 1998; Peng et al., 2005). However, increased eolian activity due to a drier climate could also increase coarse grain size fraction in lake sediment.

Contents of C and N may be the signal of primary productivity, with high values indicating high primary productivity in or around the lake and thus warm climatic conditions. Different sources of organic matter may have distinctly different  $(\text{C}/\text{N})_{\text{atomic}}$  ratios (Meyers, 1994). For example,  $(\text{C}/\text{N})_{\text{atomic}}$  ratios are generally higher in terrestrial plants, typically 20 and greater, and lower in aquatic plants, typically between 4 and 10 (Meyers, 1994). Therefore,  $(\text{C}/\text{N})_{\text{atomic}}$  ratios have the potential to provide information about the relative amounts of organic material derived from different sources (Lamb et al., 2006), and a shift to lower values may indicate an increased input from aquatic plants.

The stable carbon isotope composition ( $\delta^{13}\text{C}$ ) of sedimentary organic matter could indicate organic sources because different

sources of organic matter may have different  $\delta^{13}\text{C}$  values. Organic matter produced from atmospheric  $\text{CO}_2$  by land plants using the  $\text{C}_3$  pathway has an average  $\delta^{13}\text{C}$  value of  $\sim -27\text{‰}$  (ranging from  $-35\text{‰}$  to  $-22\text{‰}$ ) and for those using the  $\text{C}_4$  pathway the average  $\delta^{13}\text{C}$  value is  $\sim -14\text{‰}$  (varying from  $-17\text{‰}$  to  $-9\text{‰}$ ) (O'Leary, 1988). Aquatic plants (such as algae) using dissolved  $\text{CO}_2$  as their source of carbon usually have  $\delta^{13}\text{C}$  values similar to terrestrial  $\text{C}_3$  plants while those using dissolved  $\text{HCO}_3^-$  ( $\delta^{13}\text{C} = 1\text{‰}$ ) as their carbon source typically have higher  $\delta^{13}\text{C}$  values (Meyers and Lallier-vergès, 1999). Input of isotopically light  $\text{CO}_2$  from decomposition of organic matter within the lake or from land-run-off can result in more negative  $\delta^{13}\text{C}$  values of algal OM ( $\sim -32\text{‰}$ ) (Meyers and Teranes, 2002).  $\text{C}_4$  plants are mostly warm climate grasses favored by high temperature, high light and water-stress conditions, and are commonly found in grasslands in warm regions (such as low latitudes and low altitudes) with summer precipitation but are rare in cool climates (Ehleringer, 1978; Collatz et al., 1998). Because  $\text{C}_4$  plants have much higher  $\delta^{13}\text{C}$  values than  $\text{C}_3$  plants, a shift in the  $\delta^{13}\text{C}$  of sedimentary OM to higher values may indicate an increased  $\text{C}_4$  biomass in the lake watershed. In semi-arid environments, an increase in  $\text{C}_4$  biomass may suggest an increase in temperature and/or summer precipitation, implying a shift to a relatively warmer and/or wetter climate. In humid forested environments, however, an increase in  $\text{C}_4$  grasses may indicate increased seasonal drought and thus a relatively dry climate.

The nitrogen isotope ratios ( $\delta^{15}\text{N}$ ) can also help to distinguish sources of sedimentary OM. The main nitrogen source for aquatic plants is dissolved nitrate ( $\text{NO}_3^-$ ) which is enriched in  $^{15}\text{N}$  relative to atmospheric  $\text{N}_2$  (Meyers and Teranes, 2002). As a result, the  $\delta^{15}\text{N}$  values of algae ( $+7\text{‰}$  to  $+10\text{‰}$ ) are typically higher than those of land plants ( $0.4\text{‰}$ ) (Meyers, 1997). Although the isotope fractionation during biological uptake of dissolved inorganic N is small ( $<5\text{‰}$ ) (Delwiche and Steyn, 1970; Kohl and Shearer, 1980), denitrification in anoxic environment is known to cause large isotope fractionation, resulting in an enrichment of  $^{15}\text{N}$  in the remaining  $\text{NO}_3^-$  (Delwiche and Steyn, 1970; Mariotti et al., 1981). Therefore, a shift to relatively higher  $\delta^{15}\text{N}$  values, if accompanied by a shift to lower  $(\text{C}/\text{N})_{\text{atomic}}$  ratio, would indicate an increased contribution of organic matter from algae. Alternatively, if accompanied by a shift to higher  $(\text{C}/\text{N})_{\text{atomic}}$  values, higher  $\delta^{15}\text{N}$  values may indicate increased water column denitrification under anoxic conditions. Studies of land plants and soils have shown that plant  $\delta^{15}\text{N}$  values decreased with increasing mean annual precipitation (Amundson et al., 2003; De Freitas et al., 2015). Thus, a shift to higher  $\delta^{15}\text{N}$  values, if coupled with decreased regional productivity would likely indicate a shift to drier conditions. Our analysis of potential OM sources and paleoclimate condition in the study area is based on

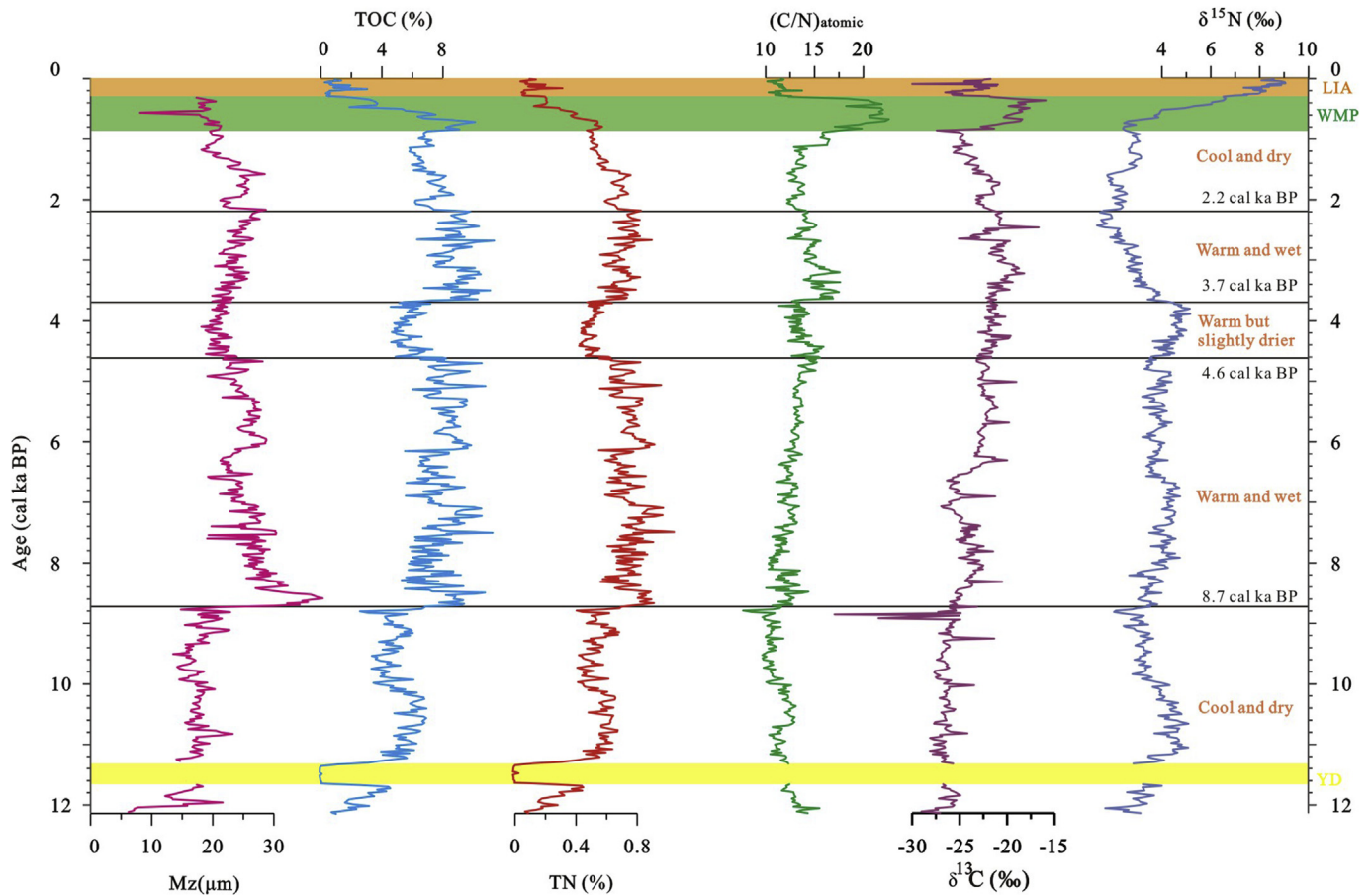


**Fig. 4.** Plots of mean grain size (Mz), content of C, N, atomic C/N ratios, and  $\delta^{13}\text{C}$ ,  $\delta^{15}\text{N}$  distribution against age. The yellow, green and orange bars denote the Younger Dryas (YD) event, Medieval Warm Period (MWP) and Little Ice Age (LIA), respectively. (For interpretation of the references to colour in this figure legend, the reader is referred to the web version of this article.)

the combination of multiple proxies as shown in Table 2.

## 5.2. Paleoenvironment reconstruction

The lithologic changes in HL-08 profile suggest that Haolaihure Paleolake experienced several environmental stages during the late Quaternary. Based on transitions of the lithology and geochemical proxies, five main paleoenvironmental stages can be distinguished (Fig. 4).

### 5.2.1. Last deglaciation to early Holocene ~12.2 cal ka BP to 8.7 cal ka BP (545–411 cm)

This stage is characterized by the deposition of black and light green clay, with a prominent eolian sand layer occurring at 526–514 cm depth that corresponds (within dating uncertainty) to the YD event (Fig. 4). The Mz values of the clay range from 6 to 23  $\mu\text{m}$ , with a mean of  $17 \pm 2.8 \mu\text{m}$ . The mean  $(\text{C}/\text{N})_{\text{atomic}}$  ratio is  $11.2 \pm 1.2$ . The relatively fine grain size and low  $(\text{C}/\text{N})_{\text{atomic}}$  ratio indicate a weak hydrodynamics in the lake watershed. The low TOC ( $4.3 \pm 1.9\%$ ) and TN ( $0.5 \pm 0.2\%$ ) in sediments suggest low productivities in the lake and its watershed. The relatively low  $\delta^{13}\text{C}$  values ( $-26.4 \pm 1.5\text{‰}$ ) and  $\delta^{15}\text{N}$  values ( $3.6 \pm 0.7\text{‰}$ ) indicate that the ecosystems consisted mainly of  $\text{C}_3$  plants, with low algae production in the lake. There is a general increasing trend in TOC, TN,  $\delta^{13}\text{C}$ , and  $\delta^{15}\text{N}$ , and a decreasing trend in  $(\text{C}/\text{N})_{\text{atomic}}$ , suggesting increasing productivity of algae during this time after 11.3 cal ka BP. These proxies suggest that the climate in the study

area was relatively cool and dry, but clearly ameliorating, during this stage (Table 2). The eolian sand layer contains very little C and N, indicating that it was formed in an extremely dry environment with little or no biomass in the area during the YD event. Taken together, these proxies suggest that the climate in the paleolake area was relatively cool and dry from ~12.2 cal ka BP to 8.7 cal ka BP, with a shift to extremely dry conditions during the YD event (Fig. 4).

### 5.2.2. Early to mid-Holocene 8.7–4.6 cal ka BP (411–225 cm)

Sediments accumulated during the time interval 8.7–4.6 cal ka BP have a mean Mz value of  $26 \pm 3.5 \mu\text{m}$ , which is larger than the mean Mz for the previous interval (Fig. 4). The increased grain size, coupled with a higher mean  $(\text{C}/\text{N})_{\text{atomic}}$  ratio of  $12.3 \pm 1.0$ , indicates an overall increase in regional runoff and erosion during this time interval compared to the previous stage. The average TOC ( $7.9 \pm 1.2\%$ ) and TN ( $0.8 \pm 0.1\%$ ) contents in sediments are also higher (Fig. 4), suggesting a generally higher regional productivity during this time period than the previous stage. The  $\delta^{13}\text{C}$  values of sedimentary organic matter are  $-23.5 \pm 1.4\text{‰}$ , about 3‰ higher than those of the previous stage (Fig. 4). This positive shift in  $\delta^{13}\text{C}$  suggests an increase in  $\text{C}_4$  biomass in a  $\text{C}_3$ -dominated environment and thus higher temperatures compared to the previous period. Slightly higher  $\delta^{15}\text{N}$  ( $3.9 \pm 0.4\text{‰}$ ) values during this time period may be caused by increased water column denitrification under anoxic conditions thus a higher lake level. All proxies indicate a relatively warm and wet climate in the area during this stage (Table 2).

**Table 2**  
Interpretations of multi-proxies.

Mz shift	TOC shift	TN shift	(C/N) <sub>atomic</sub> shift	δ <sup>13</sup> C shift	δ <sup>15</sup> N shift	Interpretation
–	–	–	–	–	–/+	Cool & dry (reduced regional productivity & runoff/terrestrial input)
+	+	+	+	+	–/+	Warm & wet (increased regional productivity, runoff/terrestrial input & C <sub>4</sub> biomass)
–	–	–	+	+	+	Warm & less humid (reduced algal input & regional productivity but with increased C <sub>4</sub> biomass & runoff)
–	+	+	+	+	+	Warm, wet & lake expansion (increased lake level, denitrification & regional productivity)

### 5.2.3. Mid Holocene 4.6–3.7 cal ka BP (225–159 cm)

A decrease in grain size ( $21 \pm 1.2 \mu\text{m}$ ), TOC ( $5.9 \pm 0.9\%$ ) and TN ( $0.5 \pm 0.1\%$ ) suggests a reduction in regional runoff and biological productivity, and thus a drier and possibly cooler regional climate from 4.6 to 3.7 cal ka BP compared to the previous stage. A shift to drier conditions is also supported by increased δ<sup>15</sup>N value ( $4.5 \pm 0.4\text{‰}$ ), which could be the result of decreased precipitation (Amundson et al., 2003; De Freitas et al., 2015). However, the mean δ<sup>13</sup>C ( $-21.6 \pm 0.7\text{‰}$ ) is higher than that of the previous stage (Fig. 4), which suggests increased C<sub>4</sub> biomass in the region. Since C<sub>4</sub> plants are mostly warm-season grasses favored by high temperature, high light and water-stress conditions while all trees and most shrubs are C<sub>3</sub> plants (Ehleringer, 1978; Collatz et al., 1998), the continued C<sub>4</sub> expansion likely occurred at the cost of reduced forest cover due to increased seasonal drought in the region. Another possibility for higher δ<sup>13</sup>C is enhanced “water-use efficiency” for C<sub>3</sub> plants (Wang et al., 2013b) and increased dissolved HCO<sub>3</sub><sup>-</sup> (Meyers and Lalliervergés, 1999) under dry and warm climatic conditions.

Increased (C/N)<sub>atomic</sub> ratios ( $13.6 \pm 1.0$ ) suggest that a larger fraction of the sedimentary organic matter was derived from land plants compared to the previous stage. Therefore, these various proxies, taken together, suggest that the environment during this stage was still warm but slightly drier than the previous stage (Table 2).

### 5.2.4. Late Holocene period after 3.7–2.2 cal ka BP (159–90 cm)

The mean Mz value ( $24 \pm 1.9 \mu\text{m}$ ) and (C/N)<sub>atomic</sub> ratio ( $14.7 \pm 1.1$ ) of sediments accumulated during this stage are greater than the mean values for the previous stage (Fig. 4), which indicate an increased regional runoff and terrestrial plant input. The TOC ( $8.9 \pm 1.0\%$ ), TN ( $0.7 \pm 0.1\%$ ), and δ<sup>13</sup>C ( $-20.9 \pm 1.3\text{‰}$ ) values also increased, suggesting an increased regional productivity and continued expansion of C<sub>4</sub> grasses during this time interval (Fig. 4). The negative shift in δ<sup>15</sup>N ( $2.7 \pm 0.6\text{‰}$ ) likely indicates a shift to wetter conditions resulting in lower δ<sup>15</sup>N of organic matter derived from terrestrial plants (Amundson et al., 2003; De Freitas et al., 2015). Thus, the multi-proxy evidence suggests a warm and wetter regional climate during this stage compared to the previous stage (Table 2).

### 5.2.5. Late Holocene period after 2.2 cal ka BP (90–0 cm)

There was a general shift to lower values of all proxies in sediments deposited in the early part of this stage, from 90 cm to 47 cm depth, relative to the previous stage (Fig. 4). The decrease in the average grain size ( $22 \pm 2.5 \mu\text{m}$ ) and (C/N)<sub>atomic</sub> ratio ( $13.7 \pm 1.4$ ) suggests decreased regional runoff and thus a drier climate compared to the previous stage. The reduced TOC ( $7.0 \pm 0.7\%$ ) and TN ( $0.6 \pm 0.1\%$ ) contents in sediments, on the other hand, suggest a lower productivity during this time interval. The lower δ<sup>13</sup>C ( $-23.3 \pm 1.5\text{‰}$ ) and δ<sup>15</sup>N ( $2.5 \pm 0.4\text{‰}$ ) indicate decreased C<sub>4</sub> biomass and algae input. Together, these proxies suggest that the early part of this stage, from ~2.2 to 0.8 cal ka BP, was characterized by relatively cool and dry climatic conditions compared to the previous stage (Table 2).

The late part of this stage was marked by two large shifts in all

proxies (Fig. 4). From 47 to 30 cm depth (~0.8–~0.3 cal yr BP), there was a sharp increase in TOC, TN, (C/N)<sub>atomic</sub> ratio, δ<sup>13</sup>C and δ<sup>15</sup>N, suggesting an increased regional productivity and runoff, coupled with increased C<sub>4</sub> biomass and anoxic water conditions. The reduction in grain size was probably the result of lake expansion that prevented coarse grain from being deposited in the center of the lake. Thus, it was a warm and wet period from ~0.8 to ~0.3 cal yr BP. After that, the Haolaihure Paleolake began to dry up and lake sediment was covered with eolian sand, which had low TOC, TN, (C/N)<sub>atomic</sub> ratio and δ<sup>13</sup>C values, indicating cooler and drier regional climate relative to the previous intervals (Fig. 4). The abnormally high δ<sup>15</sup>N values of organic matter in the eolian sand are indicative of much drier climate as the δ<sup>15</sup>N values of plants and soil generally increase with decreasing annual precipitation (Amundson et al., 2003; De Freitas et al., 2015). The warm and wet period observed during the late Holocene in the Haolaihure paleolake record can be correlated to the ‘Medieval Warm Period’ (MWP, 1000 CE – 1300 CE) within dating errors (IPCC, 2007). Considering no obvious erosion between the lacustrine sediment and the overlying sand layer, we believe the time of the cool and dry interval could probably be the ‘Little Ice Age’ (LIA, 1400– CE 1900 CE; IPCC, 2007).

### 5.3. Comparison with other regional records

This history of paleoenvironmental variation shows consistency with diatom result of the same profile from Guan et al. (2010) (with 10 cm sampling interval), but with a much higher resolution. Liu et al. (2002) also reconstructed a paleoclimate history for the Haolaihure Paleolake (also called Haoluku Paleolake) area, based on only four <sup>14</sup>C dates and subsample analysis (geochemistry and pollen) of sediments with a 5–6 cm sampling interval. The mean resolution of their record is ~200 years and radiocarbon reservoir effect was not considered. Yang et al. (2015) investigated 6 sections in and around Haolaihure Paleolake and suggested high lake levels from 10.0 ka to 5.2 ka but with no good age control.

Our multi-proxy record reveals a relatively cool and dry environment during the last deglaciation to the early Holocene with a clear warming trend after ~11.3 cal ka BP in the Haolaihure Paleolake region (Fig. 4). Our data also show that the region experienced warm and wet condition from ~8.7–2.2 cal ka BP, with a slightly drier interval at ~4.6–3.7 cal ka BP. After 2.2 cal ka BP, there was a general drying trend punctuated by a shift to warm and wet conditions during the MWP (Fig. 4). Our proxy record of climate evolution during the early and mid-Holocene in the Haolaihure Paleolake area is similar to other proxy paleoclimate records within the ASM region (Fig. 5). For examples, the proxy data from Lake Xiarinur showed that there were significant increases in pollen and *Pediastrum* concentrations at ~11.7 cal ka BP (Tang et al., 2015). Climate began to ameliorate at 10.6–10.5 cal ka BP in Bai Nuur, southeastern Inner Mongolia Plateau (Wang et al., 2012). Feng et al. (2006) summarized the records in the Inner Mongolian Plateau and suggested that the environment was generally warm and wet from ~7.5 to ~3.5 cal ka BP with an optimum at ~6.3–3.8 cal ka BP. A warm and wet climate was inferred for the Daihai Lake area from 8.1 to 3.3 cal ka BP with a relatively lower TOC at ~4.5–3.3 cal ka BP

(Xiao et al., 2006). Formation of palaeosols in Otindag Desert between 9.6 ka and 3 ka also suggested a much wetter stage during early and mid-Holocene (Yang et al., 2013). These records are consistent with the  $\delta^{18}\text{O}$  record from the Dongge Cave, which shows a prominent shift after the YD event to lower values in the early and middle Holocene, reaching the lowest values between 8 and 9 ka BP, and then an abrupt positive shift at  $\sim 3.6$  ka BP (Dykoski et al., 2005). The similarity between our record and other proxy records in the region for the early to mid-Holocene suggests that the climatic conditions in the Haolaihure Paleolake area were primarily controlled by variations in the ASM prior to 3.7 cal ka BP (Fig. 5).

In the late Holocene, our record shows a climatic amelioration in Haolaihure Paleolake area from 3.7 to 2.2 cal ka BP, which is inconsistent with the Dongge Cave  $\delta^{18}\text{O}$  record (Fig. 5). As shown in Fig. 1, the study region is located the transitional zone between the Westerlies and ASM regimes, and is sensitive to variations in both of these two climate systems. Chen et al. (2008) reviewed 11 lake sediment records in the Westerlies region in central Asian and found a shift to wetter conditions in the late Holocene between  $\sim 5$  cal ka BP and  $\sim 2$  cal ka BP (Fig. 5), opposite to that

observed in the ASM region (Dykoski et al., 2005). The persistence of wet climatic conditions after 3.7 cal ka BP seen in our record in the Inner Mongolia Plateau may be due to the strengthening of the Westerlies. The highest lake level period in the Dali Lake record was from 9.8 to 7.1 cal ka BP, which was thought to be the result of the strengthened ASM. But the low lake levels, with a rising trend, in Dali Lake from 7.1 cal ka BP until 1.8 cal ka BP (Xiao et al., 2008, 2009; Liu et al., 2015) is inconsistent with the gradual weakening of the ASM documented in the Dongge Cave  $\delta^{18}\text{O}$  record, which is, however, similar to our record from the Haolaihure Paleolake. This environmental amelioration is also recorded in Hulun Lake at about 3.35–2.0 cal ka BP (Wen et al., 2010; Zhai et al., 2011), and Juyan Lake (Herzschuh et al., 2004; Chen et al., 2008), but not seen in other records from areas located south of our study area such as Daihai Lake (Xiao et al., 2006), Huangqihai Lake (Zhang et al., 2011) and Anguli-nuur Lake (Wang et al., 2010). Although this regional inconsistency may be in part due to dating error, analysis resolution and the sensitivity of different proxy, it likely reflects the dynamic interplay of the ASM and the Westerlies in controlling the locations of the boundary between these two climate systems and thus precipitation in this region (Fig. 6).

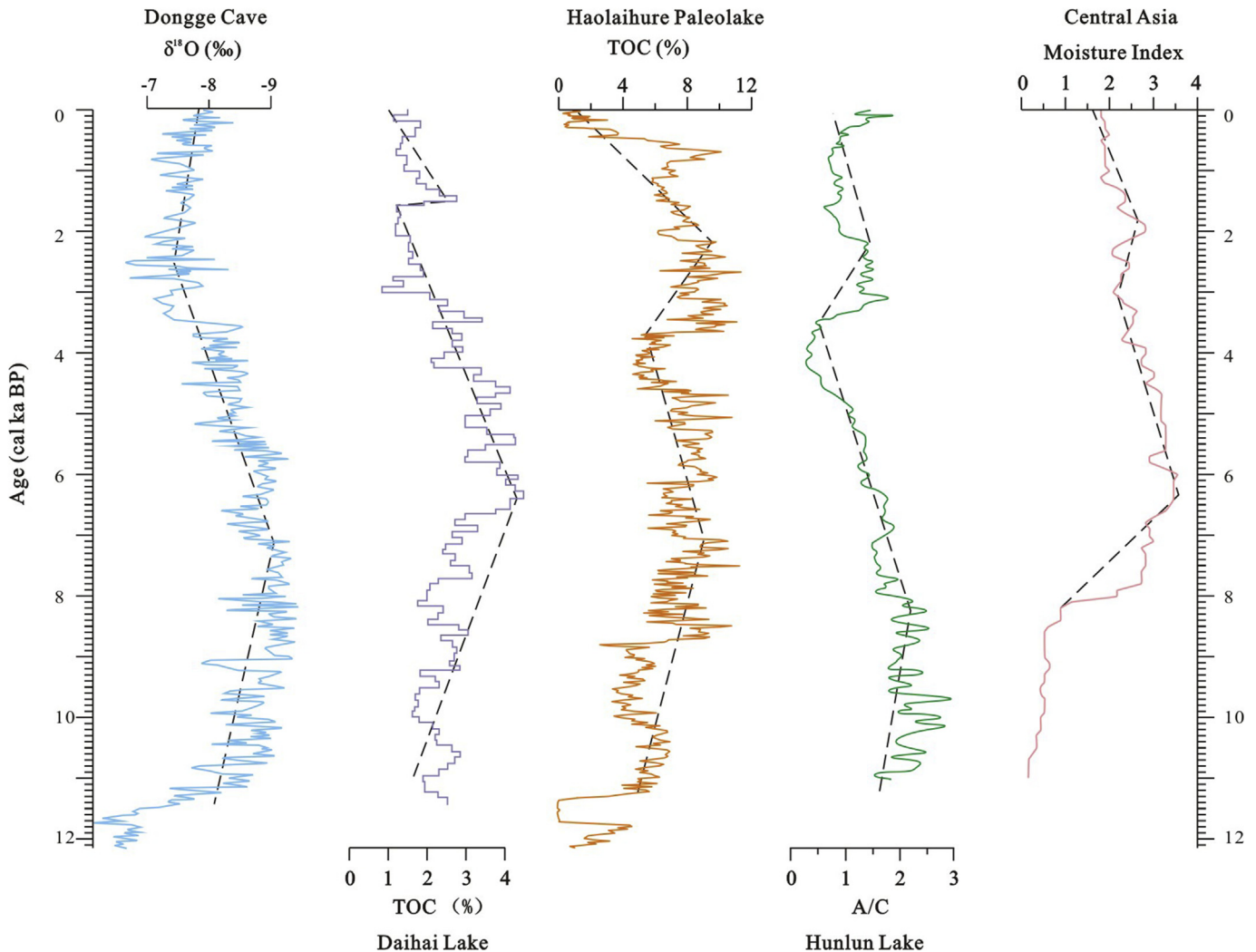


**Fig. 5.** Comparison of the Haolaihure Paleolake TOC record with other regional records (Xiao et al., 2006; Wen et al., 2010) in Inner Mongolia, speleothem  $\delta^{18}\text{O}$  record from Dongge Cave (Dykoski et al., 2005), and the central Asia moisture index (Chen et al., 2008). The dash lines indicate the trend of proxies change. The Haolaihure Paleolake record (using TOC as an example) and Hulun Lake record (A/C, ratios of *Artemisia* to *Chenopodiaceae*) are similar to those from Daihai Lake and Dongge Cave in early and mid-Holocene, but to the central Asia moisture index record in late Holocene.

The deteriorating trend after 2.2 cal ka BP is also observed in proxy records from other lakes in the ASM-Westerly transitional region including Hulun Lake (Wen et al., 2010; Zhai et al., 2011), Daihai Lake (Xiao et al., 2006), Huangqihai Lake (Zhang et al., 2011) and Anguli-nuur Lake (Wang et al., 2010). This trend is opposite to the slightly increasing trend in the ASM strength recorded in the Dongge Cave speleothems (Dykoski et al., 2005) and the Jingpo Lake sediments (Chen et al., 2015), but consistent with the central Asia record (Fig. 5). This suggests that the Westerlies probably had an increased impact in this transitional region in the latest Holocene.

The multi-proxy record from Haolaihure Paleolake reveals eight cool and dry climatic events, occurring around 0.3 (LIA), 1.3, 2.9, 4.4, 7.9, 8.9, 9.5 and 11.6 cal ka BP (YD) (Fig. 7). During these events, the grain size, TOC, TN and (C/N)<sub>atomic</sub> ratio all experienced negative shifts, indicating decreased regional productivity and runoff, and thus a cool and dry environment (Table 2, Fig. 7). This is supported by the  $\delta^{13}\text{C}$  data suggesting decreased  $\text{C}_4$  biomass during these intervals. The slight increase in  $\delta^{13}\text{C}$  at ~7.9 cal ka BP was probably the result of rapidly decreasing  $\text{C}_3$  forests in the region. The increase in  $\delta^{15}\text{N}$  at 0.3, 1.3, 2.9, 4.4 and 7.9 cal ka BP also suggest decreased input of terrestrial OM into the lake. The very negative  $\delta^{13}\text{C}$  values (~-37‰) at 8.9 cal ka BP may be due to increased decomposition/recycling of OM and consequently more  $^{13}\text{C}$ -depletion in algae. For the events at 8.9 and 9.5 cal ka BP, the decreased  $\delta^{15}\text{N}$  values were probably the result of a reduction in water column denitrification. All of these events are indicative of weak monsoon periods. The LIA and YD events have been widely reported in this region (Wang et al., 2010; Zhang et al., 2012) and other parts of China (Ma et al., 2012). The cold periods around 0.3, 1.3 and 2.9, 8.9 and 9.5 cal ka BP were also documented in Northwest China (Chen et al., 2001). The other major event around 4.4 cal ka BP has been

reported at various localities and are thought to coincide, within date error, with the collapse of the Neolithic Culture in China (NCC) (Wu and Liu, 2004; Wang et al., 2005b). The events around 1.3, 2.9, 4.4, 8.9 and 9.5 cal ka BP match well with the cold events evidenced in the record from the Tibetan Plateau (Zhou et al., 2002). The event at ~8.9 cal ka BP also coincides with the cooling of Arabian Sea around 8.8 ka BP proposed by Sirocko et al. (1993), which could have resulted in a reduction in the ISM strength. The other six events at 0.3, 1.3, 2.9, 4.4, 7.9 and 9.5 cal ka BP correlate well with the ice-rafting events in the North Atlantic (Fig. 7; Bond et al., 2001). Dongge Cave also witnessed several weak monsoon events during the Holocene that are correlated with the ice-rafting events 0–5, suggesting a possible link between the two systems (Dykoski et al., 2005; Wang et al., 2005b). This relationship has also been observed in Northwest China and Tibet Plateau (Chen et al., 2001; Zhou et al., 2002; Kelly et al., 2006; An et al., 2015). Modeling studies suggest that the ice sheet-induced cooling of the North Atlantic will cause southward displacement of the intertropical convergence zone (ITCZ) and thus reduce the monsoon strength (Broccoli et al., 2006; Zhang et al., 2010; An et al., 2015). During the late Holocene when the Westerlies appeared to be the major climatic control in the study area, cooler temperatures in the North Atlantic Ocean resulting from large meltwater discharges from the ice-sheets may also have decreased the influence of the westerlies on local precipitation (Chen et al., 2008).

## 6. Conclusion

Physical and geochemical proxies (including grain size,  $\delta^{13}\text{C}$ ,  $\delta^{15}\text{N}$ , TOC, TN and C/N) preserved in lacustrine sediments of Haolaihure Paleolake in the east central Inner Mongolia provide a nearly continuous record of paleoclimate variations over the last

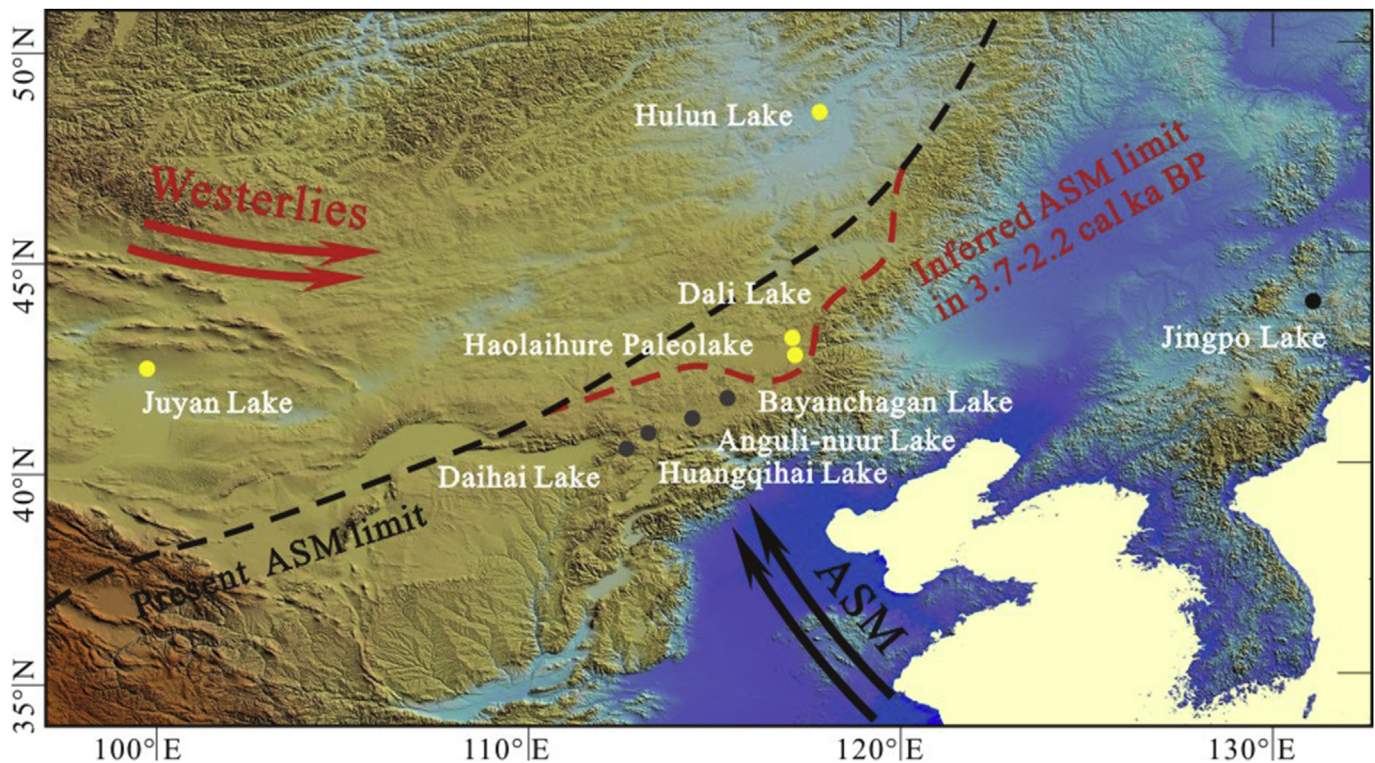
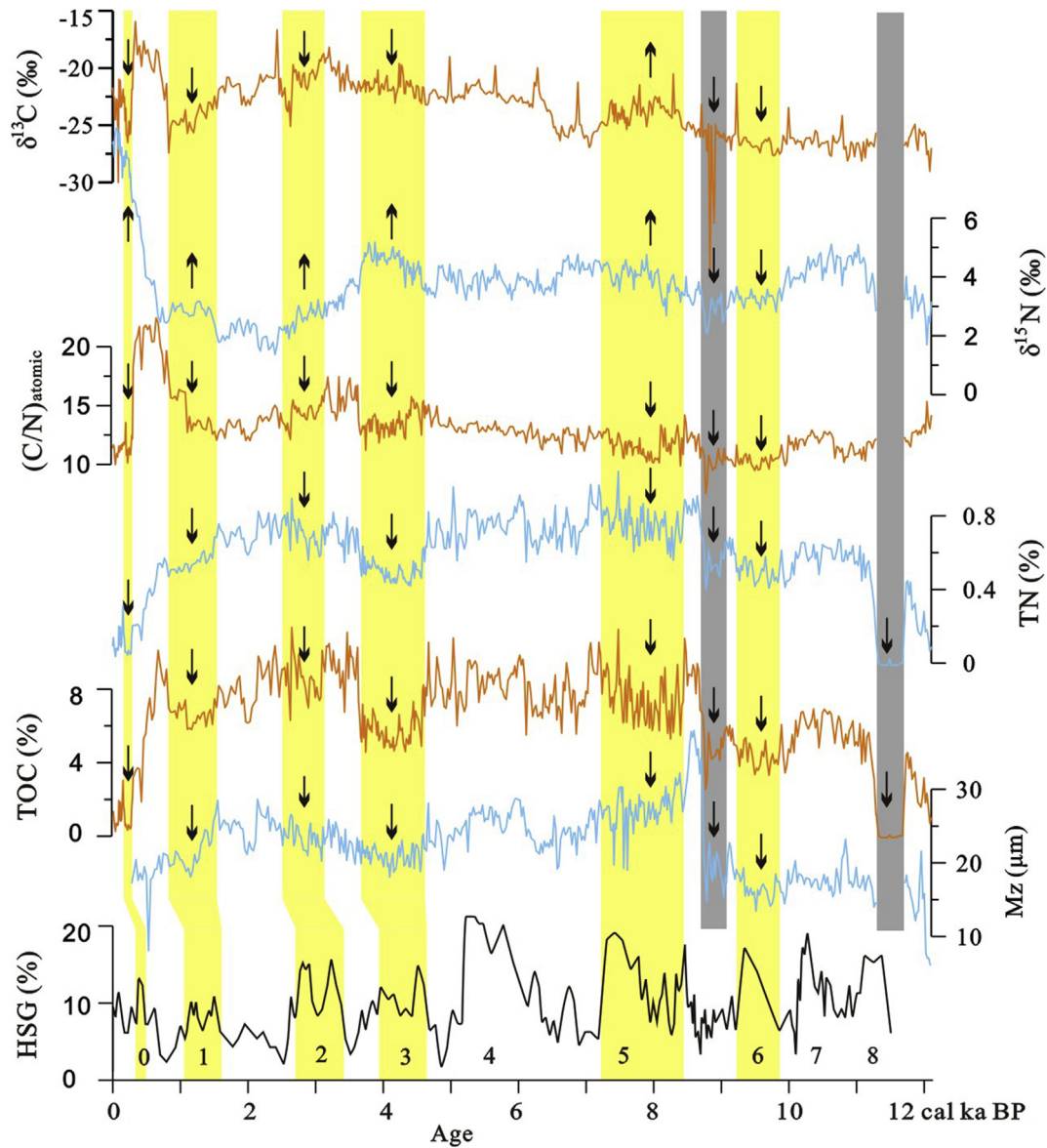


Fig. 6. Map showing the locations of the regional lakes used to compare with Haolaihure Paleolake. Yellow dots mark lakes where proxy records show a climatic amelioration at 3.7–2.2 cal ka BP in the late Holocene. Black dash line is the present ASM limit from Gao (1962). The red dash line is the inferred ASM limit at 3.7–2.2 cal ka BP (see text for discussion). (For interpretation of the references to colour in this figure legend, the reader is referred to the web version of this article.)



**Fig. 7.** Comparison of the Haolaihure Paleolake geochemical proxy records with the North Atlantic ice-raifting events (0–8) recorded by hematite stained grains (HSG) (Bond et al., 2001). The yellow and grey bars mark the cool and dry intervals in the Haolaihure Paleolake record, and the yellow ones corresponding with the ice-raifting events in the North Atlantic. (For interpretation of the references to colour in this figure legend, the reader is referred to the web version of this article.)

12,000 years. From 12.2 to 8.7 cal ka BP, the record suggests a relatively cool and dry climate in the area with an obvious amelioration after the YD event. From 8.7 to 2.2 cal ka BP, the climate was relatively warm and wet, interrupted by a brief period of slightly drier and perhaps cooler conditions at 4.6–3.7 cal ka BP. The latest Holocene after 2.2 cal ka BP was characterized by greatly deteriorating conditions with an overall cooler and drier climate. The multi-proxy record from Haolaihure Paleolake also shows a brief return to relatively warm and wet conditions during the MWP and severe drought conditions during the YD event.

Comparison of the Haolaihure Paleolake record with other proxy paleoclimate records from the region suggests that the ASM and the Westerlies both are important in controlling the environmental conditions in the east central Inner Mongolia. The climatic variations in the Haolaihure Paleolake area displayed a similar pattern to the Dongge Cave in the early to mid-Holocene and to the central Asia in the late Holocene. Six of the cool and dry climate events observed in the Haolaihure Paleolake record correlate well

with the ice-raifting events in the North Atlantic that likely resulted in a reduction in the strength of the ASM and Westerlies.

#### Acknowledgments

We thank two anonymous referees for valuable comments and suggestions that helped improve the early version of the manuscript. This study was financially supported by the Grants from the Geological Investigation Projects of China Geological Survey (Nos. 12120113005600, 1212011120142, 121201102000150010-01), and China Scholarship Council (CSC). The geochemical work was performed at the National High Magnetic Field Laboratory, which is supported by National Science Foundation Cooperative Agreement No. DMR-1157490 and the State of Florida.

#### References

Amundson, R., Austin, A.T., Schuur, E.A.G., Yoo, K., Matzek, V., Kendall, C.,

- Uebersax, A., Brenner, D., Baisden, W.T., 2003. Global patterns of the isotopic composition of soil and plant nitrogen. *Glob. Biogeochem. Cycles* 17 (1), 1031.
- An, Z.S., Porter, S.C., Kutzbach, J.E., Xi Hao, W., Su Ming, W., Xiao Dong, L., Xiao Qiang, L., Wei Jian, Z., 2000. Asynchronous Holocene optimum of the east Asian monsoon. *Quat. Sci. Rev.* 19 (8), 743–762.
- An, Z.S., Wu, G.X., Li, J.P., Sun, Y.B., Liu, Y.M., Zhou, W.J., Cai, Y.J., Duan, A.M., Li, L., Mao, J.Y., Cheng, H., Shi, Z.G., Tan, L.C., Yan, H., Ao, H., Chang, H., Feng, J., 2015. Global monsoon dynamics and climate change. *J. Earth Environ. (06)*, 341–381 (in Chinese, with English Abstract).
- Bond, G., Showers, W., Cheseby, M., Lotti, R., Almasi, P., DeMenocal, P., Priore, P., Cullen, H., Hajdas, I., Bonani, G., 1997. A pervasive millennial-scale cycle in North Atlantic Holocene and glacial climates. *Science* 278 (5341), 1257–1266.
- Bond, G., Kromer, B., Beer, J., Muscheler, R., Evans, M.N., Showers, W., Hoffmann, S., Bond, R.L., Hajdas, I., Bonani, G., 2001. Persistent solar influence on North Atlantic climate during the Holocene. *Science* 294 (5549), 2130–2136.
- Broccoli, A.J., Dahl, K.A., Stouffer, R.J., 2006. Response of the ITCZ to northern hemisphere cooling. *Geophys. Res. Lett.* 33 (1).
- Broecker, W.S., Andree, M., Wolfli, W., Oeschger, H., Bonani, G., Kennett, J., Peteet, D., 1988. The chronology of the last deglaciation: implications to the cause of the younger Dryas event. *Paleoceanography* 3 (1), 1–19.
- Campbell, C., 1998. Late Holocene lake sedimentology and climate change in southern Alberta, Canada. *Quat. Res.* 49 (1), 96–101.
- Chen, F.H., Zhu, Y., Li, J.J., 2001. Abrupt Holocene changes of the Asian monsoon at millennial-and centennial-scales: evidence from lake sediment document in Minqin Basin, NW China. *Chin. Sci. Bull.* 46 (23), 1942–1947.
- Chen, F.H., Yu, Z.C., Yang, M.L., Ito, E., Wang, S.M., Madsen, D.B., Huang, X.Z., Zhao, Y., Sato, T., Birks, H.J.B., Boomer, I., Chen, J.H., An, C.B., Wünnemann, B., 2008. Holocene moisture evolution in arid central Asia and its out-of-phase relationship with Asian monsoon history. *Quat. Sci. Rev.* 27 (3–4), 351–364.
- Chen, H.F., Song, S.R., Lee, T.Q., Löwemark, L., Chi, Z.Q., Wang, Y., Hong, E., 2010. A multiproxy lake record from Inner Mongolia displays a late Holocene teleconnection between Central Asian and North Atlantic climates. *Quat. Int.* 227 (2), 170–182.
- Chen, R., Shen, J., Li, C.H., Zhang, E.L., Sun, W.W., Ji, M., 2015. Mid- to late-Holocene East Asian summer monsoon variability recorded in lacustrine sediments from Jingpo Lake, Northeastern China. *Holocene* 25 (3), 454–468.
- Chen, Y.C., Wei, D.Y., Wang, J.J., Guan, S.Z., Qian, Z.H., Yang, Q.T., Liu, Z.M., 1996. Determination and recognition of Younger Dryas and its important significance in the salt lakes sediments of Inner Mongolian. *Geol. Chem. Minerals* 18 (3), 163–169 (in Chinese, with English Abstract).
- Cheng, H., Edwards, R.L., Wang, Y., Kong, X., Ming, Y., Kelly, M.J., Wang, X., Gallup, C.D., Liu, W., 2006. A penultimate glacial monsoon record from Hulu Cave and two-phase glacial terminations. *Geology* 34 (3), 217.
- Chu, G.Q., Sun, Q., Xie, M.M., Lin, Y., Shang, W.Y., Zhu, Q.Z., Shan, Y.B., Xu, D.K., Rioual, P., Wang, L., Liu, J.Q., 2014. Holocene cyclic climatic variations and the role of the Pacific Ocean as recorded in varved sediments from northeastern China. *Quat. Sci. Rev.* 102, 85–95.
- Collatz, G.J., Berry, J.A., Clark, J.S., 1998. Effects of climate and atmospheric CO<sub>2</sub> partial pressure on the global distribution of C<sub>4</sub> grasses: present, past, and future. *Oecologia* 114, 411–454.
- Dai, F.N., 1988. The relationship between sedimentary environments and features of surface textures of quartz sand in sand dunes of desert areas in Northern China. *J. Arid Land Resour. Environ.* (02), 25–35 (in Chinese, with English Abstract).
- Das, O., Wang, Y., Donoghue, J., Xu, X., Coor, J., Elsner, J., Xu, Y., 2013. Reconstruction of paleostorms and paleoenvironment using geochemical proxies archived in the sediments of two coastal lakes in northwest Florida. *Quat. Sci. Rev.* 68, 142–153.
- De Freitas, A.D.S., de Sá Barretto Sampaio, E.V., de Souza Ramos, A.P., de Vasconcellos Barbosa, M.R., Lyra, R.P., Araújo, E.L., 2015. Nitrogen isotopic patterns in tropical forests along a rainfall gradient in Northeast Brazil. *Plant Soil* 391 (1–2), 109–122.
- Delwiche, C.C., Steyn, P.L., 1970. Nitrogen isotope fractionation in soils and microbial reactions. *Environ. Sci. Technol.* 4, 929–935.
- Dykoski, C.A., Edwards, R.L., Cheng, H., Yuan, D.X., Cai, Y.J., Zhang, M.L., Lin, Y.S., Qing, J., An, Z.S., Revenaugh, J., 2005. A high-resolution, absolute-dated Holocene and deglacial Asian monsoon record from Dongge Cave, China. *Earth Planet. Sci. Lett.* 233, 71–86.
- Ehleringer, J.R., 1978. Implications of quantum yield differences on the Distributions of C<sub>3</sub> and C<sub>4</sub> grasses. *Oecologia* 31, 255–267.
- Feng, Z.D., An, C.B., Wang, H.B., 2006. Holocene climatic and environmental changes in the arid and semi-arid areas of China: a review. *Holocene* 16 (1), 119–130.
- Gao, Y.X., 1962. Some Problems on East-Asia Monsoon. Science Press, Beijing (in Chinese).
- Guan, Y.Y., Wang, Y., Yao, P.Y., Chi, Z.Q., Zhao, Z.L., 2010. Environmental evolution since the Holocene in the haolaihu ancient lake, Keshiketengqi, Inner Mongolia, China. *Geol. Bull. China* 29 (6), 891–900 (in Chinese, with English Abstract).
- Håkanson, L., Jansson, M., 1983. Principles of Lake Sedimentology. Springer, Berlin.
- Herzschuh, U., Tarasov, P., Wünnemann, B., Hartmann, K., 2004. Holocene vegetation and climate of the Alashan Plateau, NW China, reconstructed from pollen data. *Palaeogeogr. Palaeoclimatol. Palaeoecol.* 211 (1–2), 1–17.
- IPCC, 2007. Climate change 2007: the physical science basis. In: Solomon, S., Qin, D., Manning, M., Chen, Z., Marquis, M., Averyt, K.B., Tignor, M., Miller, H.L. (Eds.), Contribution of Working Group I to the Fourth Assessment Report of the Intergovernmental Panel on Climate Change. Cambridge University Press, Cambridge, United Kingdom and New York.
- Jiang, W.Y., Guo, Z.T., Sun, X.J., Wu, H.B., Chu, G.Q., Yuan, B.Y., Hatté, C., Guiot, J., 2006. Reconstruction of climate and vegetation changes of lake bayanchagan (Inner Mongolia): Holocene variability of the east Asian monsoon. *Quat. Res.* 65 (3), 411–420.
- Jiang, W.Y., Guiot, J., Chu, G.Q., Wu, H.B., Yuan, B.Y., Hatté, C., Guo, Z.T., 2010. An improved methodology of the modern analogues technique for palaeoclimate reconstruction in arid and semi-arid regions. *Boreas* 39, 145–153.
- Kelly, M.J., Edwards, R.L., Cheng, H., Yuan, D., Cai, Y., Zhang, M., Lin, Y., An, Z., 2006. High resolution characterization of the Asian Monsoon between 146,000 and 99,000 years B.P. from Dongge Cave, China and global correlation of events surrounding Termination II. *Palaeogeogr. Palaeoclimatol. Palaeoecol.* 236 (1–2), 20–38.
- Kohl, D.H., Shearer, G., 1980. Isotopic fractionation Associated with symbiotic N<sub>2</sub> fixation and uptake of NO<sub>3</sub>– by plants. *Plant Physiol.* 66, 51–56.
- Krinsley, D., Margolis, S., 1969. Section of geological sciences: a study of quartz sand grain surface textures with the scanning electron microscope. *Trans. N. Y. Acad. Sci.* 31 (5 Series II), 457–477.
- Lamb, A.L., Wilson, G.P., Leng, M.J., 2006. A review of coastal palaeoclimate and relative sea-level reconstructions using  $\delta^{13}C$  and C/N ratios in organic material. *Earth Sci. Rev.* 75 (1–4), 29–57.
- Li, Z.G., 1993. Annals of Hexigten Banner. People's Press of Inner Mongolia, Hohhot (in Chinese).
- Liu, H.Y., Xu, L.H., Cui, H.T., 2002. Holocene history of desertification along the woodland-steppe border in northern China. *Quat. Res.* 57 (2), 259–270.
- Liu, K., 1988. Quaternary history of the temperate forests of China. *Quat. Sci. Rev.* 7, 1–20.
- Liu, S.Z., Deng, C.L., Xiao, J.L., Li, J.H., Paterson, G.A., Chang, L., Yi, L., Qin, H.F., Pan, Y.X., Zhu, R.X., 2015. Insolation driven biomagnetic response to the Holocene warm period in semi-arid East Asia. *Sci. Rep.* 5, 8001.
- Liu, X.Q., Dong, H.L., Rechb, J.A., Matsumoto, R., Yang, B., Wang, Y.B., 2008. Evolution of chaka salt lake in NW China in response to climatic change during the latest pleistocene – Holocene. *Quat. Sci. Rev.* 27, 867–879.
- Long, H., Shen, J., Wang, Y., Gao, L., Frechen, M., 2015. High-resolution OSL dating of a late quaternary sequence from xingkai lake (NE Asia): chronological challenge of the “MIS 3a mega-paleolake” hypothesis in China. *Earth Planet. Sci. Lett.* 428, 281–292.
- Lorente, F.L., Pessenda, L.C.R., Oboh-Ikenobe, F., Buso Jr., A.A., Cohen, M.C.L., Meyer, K.E.B., Giannini, P.C.F., de Oliveira, P.E., Rossetti, D.D.F., Borotti Filho, M.A., Franca, M.C., de Castro, D.F., Bendassolli, J.A., Macario, K., 2014. Palynofacies and stable C and N isotopes of Holocene sediments from Lake macuco (Linhares, Espírito Santo, southeastern Brazil): depositional settings and palaeoenvironmental evolution. *Palaeogeogr. Palaeoclimatol. Palaeoecol.* 415, 69–82.
- Lukas, S., Preusser, F., Anselmetti, F.S., Tinner, W., 2012. Testing the potential of luminescence dating of high-alpine lake sediments. *Quat. Geochronol.* 8, 23–32.
- Ma, Z.B., Cheng, H., Tan, M., Edwards, R.L., Li, H.C., You, C.F., Duan, W.H., Wang, X., Kelly, M.J., 2012. Timing and structure of the Younger Dryas event in northern China. *Quaternary Sci. Rev.* 41, 83–93.
- Mahaney, W.C., 2002. Atlas of Sand Grain Surface Textures and Applications. Oxford University Press, USA.
- Mariotti, A., Germon, J.C., Hubert, P., Kaiser, P., Letolle, R., Tardieu, A., Tardieu, P., 1981. Experimental determination of nitrogen kinetic isotope fractionation: some principles; illustration for the denitrification and nitrification processes. *Plant Soil* 62, 413–430.
- Meyers, P.A., 1994. Preservation of elemental and isotopic source identification of sedimentary organic matter. *Chem. Geol.* 114, 289–302.
- Meyers, P.A., 1997. Organic geochemical proxies of paleoceanographic, paleolimnologic, and paleoclimatic processes. *Org. Geochem.* 27, 213–250.
- Meyers, P.A., Lallier-vergès, E., 1999. Lacustrine sedimentary organic matter records of late quaternary paleoclimates. *J. Paleolimnol.* 21 (3), 345–372.
- Meyers, P.A., Teranes, J.L., 2002. Sediment organic matter. In: S. J. E., Last, W.M. (Eds.), Tracking Environmental Change Using Lake Sediments. Volume 2 of the Series Developments in Paleoenvironment Research. Kluwer-Academic, Dordrecht, Netherlands, pp. 239–269.
- Muscheler, R., Kromer, B., Björck, S., Svensson, A., Friedrich, M., Kaiser, K.F., Southon, J., 2008. Tree rings and ice cores reveal 14C calibration uncertainties during the Younger Dryas. *Nat. Geosci.* 4, 263–276.
- O'Leary, M.H., 1988. Carbon isotopes in photosynthesis. *Bioscience* 38 (5), 328–336.
- Peng, Y.J., Xiao, J.L., Nakamura, T., Liu, B.L., Inouchi, Y., 2005. Holocene East Asian monsoonal precipitation pattern revealed by grain-size distribution of core sediments of Daihai Lake in Inner Mongolia of north-central China. *Earth Planet. Sci. Lett.* 233, 467–479.
- Qian, W.H., Lin, X., Zhu, Y.F., Xu, Y., Fu, J.L., 2007. Climatic regime shift and decadal anomalous events in China. *Clim. Change* 84 (2), 167–189.
- Ramsey, C.B., 2009. Bayesian analysis of radiocarbon dates. *Radiocarbon* 51, 337–360.
- Reimer, P.J., Bard, E., Bayliss, A., Beck, J.W., Blackwell, P.G., Ramsey, C.B., Buck, C.E., Cheng, H., Edwards, R.L., Friedrich, M., 2013. IntCal13 and Marine13 radiocarbon age calibration curves 0–50,000 years cal BP. *Radiocarbon* 55, 1869–1887.
- Ren, G.Y., 1998. A finding of the influence of “hard water” on radio carbon dating for the lake sediments in Inner Mongolia, China. *J. Lake Sci.* 10, 80–82 (in Chinese, with English Abstract).
- Sirocko, F., Sarntheim, M., Erlenkeuser, H., Lange, H., Arnold, M., Duplessy, J.C., 1993. Century-scale events in monsoonal climate over the past 24000 years. *Nature*

- 364 (6435), 322–324.
- Stuiver, M., Grootes, P.M., Braziunas, T.F., 1995. The GISP2  $\delta^{18}O$  climate record of the past 16,500 years and the role of the sun, ocean, and volcanoes. *Quat. Res.* 44, 341–354.
- Sun, J.M., Li, S.H., Han, P., Chen, Y.Y., 2006. Holocene environmental changes in the central Inner Mongolia, based on single-aliquot-quartz optical dating and multi-proxy study of dune sands. *Palaeogeogr. Palaeoclimatol. Palaeoecol.* 233 (1–2), 51–62.
- Sun, X.J., Wang, P.X., 2005. How old is the Asian monsoon system?—Palaeobotanical records from China. *Palaeogeogr. Palaeoclimatol. Palaeoecol.* 222 (3–4), 181–222.
- Tang, L., Wang, X.S., Zhang, S.Q., Chu, G.Q., Chen, Y., Pei, J.L., Sheng, M., Yang, Z.Y., 2015. High-resolution magnetic and palynological records of the last deglaciation and Holocene from Lake Xiarinur in the hunshandake sandy land, Inner Mongolia. *Holocene* 25 (5), 844–856.
- Wang, G.A., Li, J.Z., Liu, X.Z., Li, X.Y., 2013b. Variations in carbon isotope ratios of plants across a temperature gradient along the 400 mm isohet of mean annual precipitation in north China and their relevance to paleovegetation reconstruction. *Quat. Sci. Rev.* 63, 83–90.
- Wang, H.Y., Liu, H.Y., Cui, H.T., Abrahamsen, N., 2001. Terminal Pleistocene/Holocene palaeoenvironmental changes revealed by mineral-magnetism measurements of lake sediments for Dali Nor area, southeastern Inner Mongolia Plateau, China. *Palaeogeogr. Palaeoclimatol. Palaeoecol.* 170 (1), 115–132.
- Wang, H.Y., Liu, H.Y., Zhu, J.L., Yin, Y., 2010. Holocene environmental changes as recorded by mineral magnetism of sediments from Anguli-nuur Lake, southeastern Inner Mongolia Plateau, China. *Palaeogeogr. Palaeoclimatol. Palaeoecol.* 285 (1–2), 30–49.
- Wang, H.Y., Liu, H.Y., Zhao, F.J., Yin, Y., Zhu, J.L., Snowball, I., 2012. Early- and mid-Holocene palaeoenvironments as revealed by mineral magnetic, geochemical and palynological data of sediments from Bai Nuur and Ulan Nuur, southeastern inner Mongolia Plateau, China. *Quat. Int.* 250, 100–118.
- Wang, K.L., Jiang, H., Zhao, H.Y., 2005a. Atmospheric water vapor transport from westerly and monsoon over the Northwest China. *Adv. Water Sci.* 16 (3), 432–438 (in Chinese, with English Abstract).
- Wang, N.A., Li, Z.L., Li, Y., Cheng, H.Y., 2013a. Millennial-scale environmental changes in the Asian monsoon margin during the Holocene, implicated by the lake evolution of Huahai Lake in the Hexi Corridor of northwest China. *Quat. Int.* 313–314, 100–109.
- Wang, S.M., Ji, L., Yang, X.D., Xue, B., Ma, Y., Hu, S.Y., 1994. The record of younger Dryas event in lake sediments from Jalai Nur, Inner Mongolia. *Chin. Sci. Bull.* 39 (10), 831–835.
- Wang, Y.J., Cheng, H., Edwards, R.L., He, Y.Q., Kong, X.G., An, Z.S., Wu, J.Y., Kelly, M.J., Dykosi, C.A., Li, X.D., 2005b. The Holocene Asian monsoon: links to solar changes and North Atlantic climate. *Science* 308 (5723), 854–857.
- Wen, R.L., Xiao, J.L., Chang, Z.G., Zhai, D.Y., Xu, Q.H., Li, Y.C., Itoh, S., Lomtatidze, Z., 2010. Holocene climate changes in the mid-high-latitude-monsoon margin reflected by the pollen record from Hulun Lake, northeastern Inner Mongolia. *Quat. Res.* 73, 293–303.
- Wu, W.X., Liu, T.S., 2004. Possible role of the “Holocene event 3” on the collapse of neolithic cultures around the central plain of China. *Quat. Int.* 117 (1), 153–166.
- Xiao, J.L., Wu, J.T., Si, B., Liang, W.D., Nakamura, T., Liu, B.L., Inouchi, Y., 2006. Holocene climate changes in the monsoon/arid transition reflected by carbon concentration in Daihai Lake of Inner Mongolia. *Holocene* 16 (4), 551–560.
- Xiao, J.L., Si, B., Zhai, D.Y., Itoh, S., Lomtatidze, Z., 2008. Hydrology of Dali Lake in central-eastern Inner Mongolia and Holocene East Asian monsoon variability. *J. Paleolimnol.* 40, 519–528.
- Xiao, J.L., Chang, Z.G., Si, B., Qin, X.G., Itoh, S., Lomtatidze, Z., 2009. Partitioning of the grain-size components of Dali Lake core sediments: evidence for lake-level changes during the Holocene. *J. Paleolimnol.* 42, 249–260.
- Yang, S.L., Ding, Z.L., Li, Y.Y., Wang, X., Jiang, W.Y., Huang, X.F., 2015. Warming-induced northward migration of the East Asian monsoon rain belt from the Last Glacial Maximum to the mid-Holocene. *Proc. Natl. Acad. Sci.* 112 (43), 13178–13183.
- Yang, X.P., Wang, X.L., Liu, Z.T., Li, H.W., Ren, X.Z., Zhang, D.G., Ma, Z.B., Rioual, P., Jin, X.D., Scuderi, L., 2013. Initiation and variation of the dune fields in semi-arid China – with a special reference to the Hunshandake Sandy Land, Inner Mongolia. *Quat. Sci. Rev.* 78, 369–380.
- Yang, X.P., Scuderi, L.A., Wang, X.L., Scuderi, L.J., Zhang, D.G., Li, H.W., Forman, S., Xu, Q.H., Wang, R.C., Huang, W.W., Yang, S.X., 2015. Groundwater sapping as the cause of irreversible desertification of Hunshandake Sandy Lands, Inner Mongolia, northern China. *Proc. Natl. Acad. Sci.* 112, 702–706.
- Zhai, D.Y., Xiao, J.L., Zhou, L., Wen, R.L., Chang, Z.G., Wang, X., Jin, X.D., Pang, Q.Q., Itoh, S., 2011. Holocene East Asian monsoon variation inferred from species assemblage and shell chemistry of the ostracodes from Hulun Lake, Inner Mongolia. *Quat. Res.* 75 (3), 512–522.
- Zhang, J.R., Jia, Y.L., Lai, Z.P., Long, H., Yang, L.H., 2011. Holocene evolution of Huangqihai Lake in semi-arid northern China based on sedimentology and luminescence dating. *Holocene* 21 (8), 1261–1268.
- Zhang, R., Kang, S.M., Held, I.M., 2010. Sensitivity of climate change induced by the weakening of the Atlantic meridional overturning circulation to cloud feedback. *J. Clim.* 23 (2), 378–389.
- Zhang, W.C., Yan, H., Cheng, P., Lu, F.Y., Li, M., Dodson, J., Zhou, W.J., An, Z.S., 2016. Peatland development and climate changes in the Dajihu basin, central China, over the last 14,100 years. *Quat. Int.* 425, 273–281.
- Zhang, X.Y., Zhou, Y.L., Pang, J.L., Lu, H.Y., Huang, C.C., Zhou, L., Gu, H.L., 2012. The relationship between environmental changes and human activities during the medieval warm period and the little ice age in Otindag sandland by OSL dating. *Quat. Sci.* 32 (3), 535–546 (in Chinese, with English Abstract).
- Zhou, W.J., Liu, X.F., Wu, Z.K., Deng, L., Jull, A.J.T., 2002. Peat record reflecting Holocene climatic change in the Zoige Plateau and AMS radiocarbon dating. *D. D. and W. B. Chin. Sci. Bull.* 47, 66–70.